Modeling of CeO_2, Ce_2O_3, and CeO_{2-x} in the LDA+U formalism

D. A. Andersson,[1] S. I. Simak,[2] B. Johansson,[1,3] I. A. Abrikosov,[2] and N. V. Skorodumova[3]
[1]*Applied Materials Physics, Department of Materials Science and Engineering, Royal Institute of Technology, SE-100 44 Stockholm, Sweden*
[2]*Department of Physics, Chemistry and Biology (IFM), Linköping University, SE-581 83 Linköping, Sweden*
[3]*Condensed Matter Theory Group, Department of Physics, Uppsala University, Box 530, SE-751 21 Uppsala, Sweden*
(Received 12 June 2006; revised manuscript received 5 October 2006; published 8 January 2007)

The electronic structure and thermodynamic properties of CeO_2 and Ce_2O_3 have been studied from first principles by the all-electron projector-augmented-wave (PAW) method, as implemented in the *ab initio* total-energy and molecular-dynamics program VASP (Vienna *ab initio* simulation package). The local density approximation (LDA)+U formalism has been used to account for the strong on-site Coulomb repulsion among the localized Ce 4f electrons. We discuss how the properties of CeO_2 and Ce_2O_3 are affected by the choice of U as well as the choice of exchange-correlation potential, i.e., the local density approximation or the generalized gradient approximation. Further, reduction of CeO_2, leading to formation of Ce_2O_3 and CeO_{2-x}, and its dependence on U and exchange-correlation potential have been studied in detail. Our results show that by choosing an appropriate U it is possible to consistently describe structural, thermodynamic, and electronic properties of CeO_2, Ce_2O_3, and CeO_{2-x}, which enables modeling of redox processes involving ceria-based materials.

DOI: 10.1103/PhysRevB.75.035109 PACS number(s): 71.15.Nc, 71.30.+h, 71.28.+d, 71.27.+a

I. INTRODUCTION

Many technological fields, e.g., solid oxide fuel cells[1] and catalysis,[2] have benefited from the unique redox and transport properties of ceria (CeO_2) and ceria-based materials. In catalytic applications the ability of ceria to release oxygen by forming oxygen vacancies under oxygen-poor (reducing) conditions and, conversely, to store oxygen by filling oxygen vacancies under oxygen-rich (oxidizing) conditions is employed to stabilize the air-to-fuel ratio at the desired level.[2] This property is related to the quantum process of electron localization and delocalization.[3–10] In CeO_2 oxygen has a formal valence of −2 (O^{2-}) and, when an oxygen atom is released, in the form of (half) an oxygen molecule, two electrons are left behind. These electrons localize on the f-level traps on two Ce atoms, which change their formal valence from +4 to +3.[3] During oxidation the reverse process occurs.

Modeling of the electron localization, and thus any redox process involving ceria, is a complex task. Conventional density functional schemes that apply different flavors of the local density approximation underestimate the strong on-site Coulomb repulsion of the Ce 4f electrons and consequently fail to capture the localization.[4–10] Therefore, the 4f electrons in elemental Ce, as well as in Ce compounds, require special attention. Using quantum mechanical calculations Skorodumova *et al.*[4] showed that the properties of Ce 4f electrons in CeO_2, i.e., the +4 modification of Ce, can be described by treating the 4f electrons as part of the valence band [the valence band model (VBM)], while localized 4f electrons in Ce_2O_3, i.e., the +3 modification of Ce, can be modeled by treating the 4f electrons as part of the core states [the core state model (CSM)]. Skorodumova *et al.*[3] have also argued that formation of vacancies in CeO_2 is accompanied by localization of two electrons on the f-level traps on two Ce atoms and that these atoms can be described within the CSM. A drawback with this approach, based on either the local density approximation (LDA) or the generalized gradient approximation (GGA), is that it is not possible to directly obtain the energetics of the redox reaction. One way to overcome this deficiency is to apply the so-called LDA+U approach,[11–13] in which the underestimation of the intraband Coulomb interactions is corrected for by the Hubbard U parameter. This method and its applications to ceria have been discussed by several authors.[5–10,14,15] The choice of U is, however, not unambiguous and it is not trivial to determine its value *a priori*, though there are attempts to extract it from standard first-principles calculations.[16,17] Hence, U is often fitted to reproduce a certain set of experimental data, for example band gaps and structural properties.

In the present work we use the LDA+U scheme due to Dudarev *et al.*[13] to calculate lattice parameters, thermodynamic properties, and band structures of CeO_2, Ce_2O_3, and CeO_{2-x}. We discuss how these properties are affected by the choice of U as well as the choice of exchange-correlation potential, i.e., the local density approximation or the generalized gradient approximation, and how redox processes that involve ceria-based materials can be accurately described in the LDA+U formalism.

The paper is organized as follows. The details of our calculations are described in Sec. II and in Sec. III we present and discuss the results. In the final part, Sec. IV, we summarize our findings.

II. THEORY

The calculations were performed using the frozen-core all-electron projector-augmented-wave (PAW) method, as implemented in the *ab initio* total-energy and molecular-dynamics program VASP (Vienna *ab initio* simulation program).[18–22] We used the LDA+U formalism formulated by Dudarev *et al.*[13] to account for the strong on-site Coulomb repulsion amongst the localized Ce 4f electrons. In this

scheme[13] the orbital-dependent LDA+U functional is of the form

$$E_{LDA+U} = E_{LDA} + \frac{U-J}{2}\sum_{\sigma}[\mathrm{Tr}\rho^{\sigma} - \mathrm{Tr}(\rho^{\sigma}\rho^{\sigma})], \qquad (1)$$

where ρ^{σ} is the density matrix of f states, and U and J are the spherically averaged screened Coulomb energy and the exchange energy, respectively. Here only the difference between U and J is significant[13] and consequently we will henceforth treat them as one single parameter, for simplicity labeled as U. We remark that in this paper we have omitted the explicit spin (S) reference in the L(S)DA+U abbreviation, i.e., we denote it as LDA+U.

The exchange and correlation effects were treated in both the local density approximation and the generalized gradient approximation.[23] We studied CeO_2 in its ground-state fluorite structure ($Fm\bar{3}m$) and the sesquioxide Ce_2O_3 in the hexagonal A-type structure ($P\bar{3}m1$). For CeO_2 we used a $13\times13\times13$ Monkhorst-Pack k-point mesh[24] (84 irreducible k points) and for Ce_2O_3 we used a $7\times7\times7$ Γ-centered grid (44 irreducible k points). The density of states (DOS) was obtained with $15\times15\times15$ (120 irreducible k points) and $9\times9\times9$ (88 irreducible k points) k-point meshes, respectively. The Brillouin-zone integration was performed using the modified tetrahedron method of Blöchl.[25] The equilibrium volume of Ce_2O_3 was determined by optimizing all internal structural parameters at constant cell volume and then minimizing the energy with respect to the cell volume. We modeled reduced ceria CeO_{2-x} using a $2\times2\times2$ supercell (96 sites), derived from an ideal fluorite structure. The volume of the supercell was assumed to be constant and equal to the calculated volume of bulk ceria. For $U=6$ eV the error due to keeping the cell volume constant is 0.04 eV, which is negligible at the energy scale of vacancy formation energies. We relaxed all internal structural parameters until the Hellmann-Feynman forces on each ion were negligible (<0.01 eV/Å). For the supercell calculations we used either a $2\times2\times2$ Monkhorst-Pack k-point mesh[24] (two irreducible k points) and Gaussian smearing with a smearing parameter of 0.20 eV or a $3\times3\times3$ Monkhorst-Pack k-point mesh[24] (eight irreducible k points) together with the modified tetrahedron method of Blöchl.[25] To assure accurate results we used a plane-wave cutoff energy of 400 eV for all calculations. In order to study vacancy formation in ceria it is necessary to estimate the chemical potential of O_2. We defined the energy of an oxygen molecule (E_{O_2}) as the energy of an isolated (noninteracting) molecule and the effect of spin polarization was included.

III. RESULTS AND DISCUSSION

A. Electronic structure of CeO_2 and Ce_2O_3

CeO_2 is an insulator with a band gap of 6 eV,[26] and the Ce 4f band is unoccupied. In Fig. 1 we plot the density of states for CeO_2 calculated with $U=0$ and 6 eV (LDA). For consistency with reduced ceria we used spin-polarized calculations also for CeO_2. The gap between the valence and conduction bands is 5.5 eV and the distance between the valence band and the Ce 4f edge is 1.9 eV, to be compared with 3 eV in experiments.[26] The width of the O 2p band is 4.2 eV, which agrees with experiments[26] and a previous theoretical study.[4] For CeO_2 the main effect of increasing U is to push up the unoccupied f band and slightly decrease the band gap, which was also observed in Ref. 9.

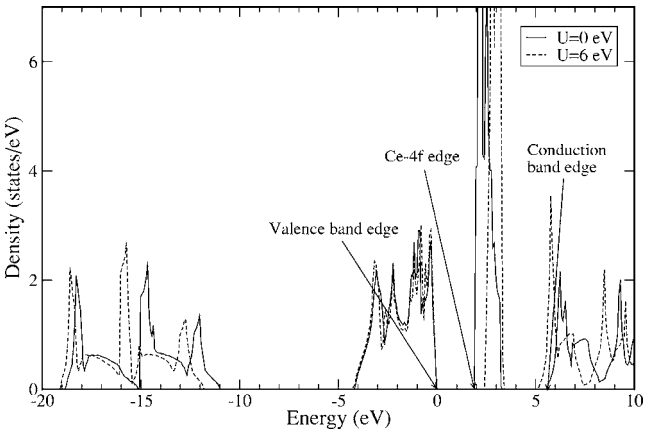

FIG. 1. The DOS of CeO_2 obtained with the LDA for $U=0$ and 6 eV. The highest occupied state is at 0 eV. The arrows indicate the band edge positions for $U=0$ eV. Since the spin-up and spin-down channels are identical, only the spin-up channel is shown.

According to experiments, deviation from ideal stoichiometry, i.e., CeO_{2-x}, leads to an occupation of the f band, which splits into an occupied part and an unoccupied part.[27–29] Hence this material is also an insulator. The occupied orbitals are localized and from experiments they are known to be situated 1.2–1.5 eV above the O 2p valence band edge.[27–29] Ce_2O_3 is the end product of the reduction process and the occupied and unoccupied f levels are separated from each other also in this case. Figures 2 and 3 show the DOS and partial DOS (PDOS) of Ce_2O_3 for $U=0$ and 6 eV (LDA). The localized f electrons must follow Hund's rules and consequently one has to allow for spin polarization. The results in Figs. 2 and 3 were obtained using antiferro-

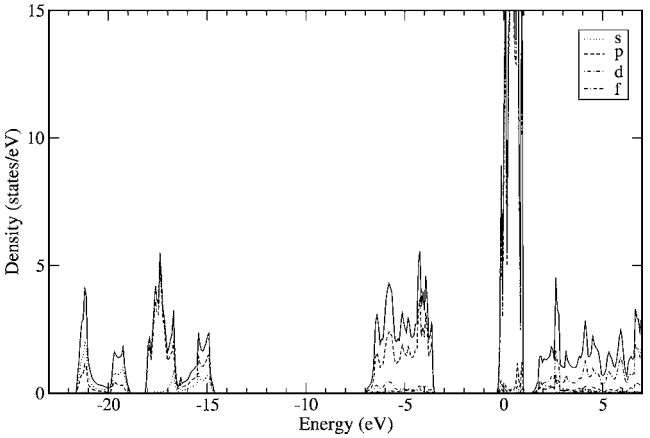

FIG. 2. The DOS (black line) and PDOS of Ce_2O_3 obtained with the LDA for $U=0$ eV. Since the spin-up and spin-down channels are identical, only the spin-up channel is shown. The highest occupied state is at 0 eV.

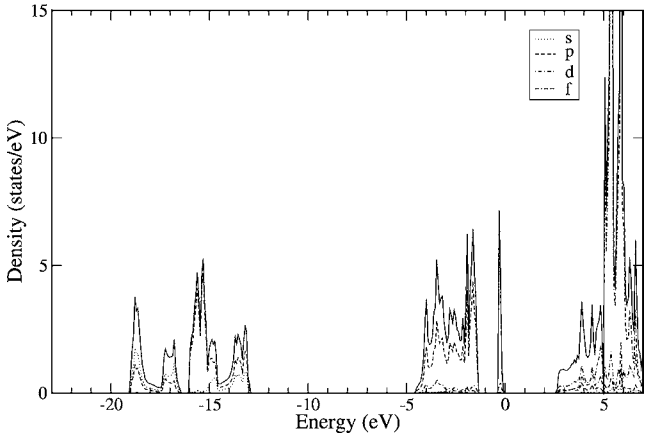

FIG. 3. The DOS (black line) and PDOS of Ce_2O_3 obtained with the LDA for $U=6$ eV. Since the spin-up and spin-down channels are identical, only the spin-up channel is shown. The highest occupied state is at 0 eV.

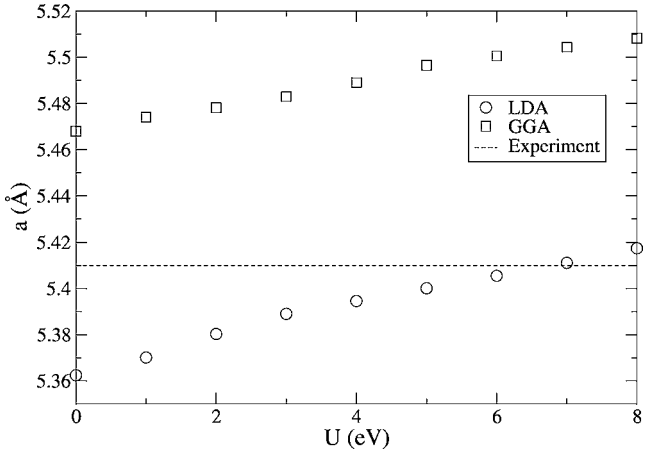

FIG. 4. The lattice parameter (a) of CeO_2 as function U. The horizontal line indicates the experimental value(Ref. 30).

magnetic (AFM) ordering of the magnetic moments. The ferromagnetic (FM) solution is 0.057 eV/Ce_2O_3 (LDA) lower in energy for $U=0$ eV, but for higher U the AFM solution is more stable. For $U=0$ eV the f band does not split for either the AFM or the FM solution and the obtained ground state is metallic (Fig. 2), which disagrees with available experiments. However, if we increase U above 2 eV the f band splits and an insulating solution with a finite separation of the occupied and unoccupied f band is found (Fig. 3). For $U=1$ eV the DOS is ≈ 0 at the Fermi level; however, there is no separation at the equilibrium volume. If the volume is increased above the calculated equilibrium volume a separation opens up at the local minimum of the DOS. Thus the exact value of U for which the transition from metallic to insulating solutions occurs depends on volume. According to Ref. 14, which applied the same computational method as in the present work, the transition value is $U=0.4$ eV. As can be seen in Fig. 3 the occupied f band is 0.95 eV above the O $2p$ valence band edge for $U=6$ eV. This distance decreases for increasing U and the occupied Ce $4f$ states will eventually merge with the O $2p$ valence band. For any U the occupied gap states move toward the O $2p$ valence band edge when the volume increases and toward the conduction band when the volume decreases. The gap between the O $2p$ valence band edge and the conduction band (mainly Ce $5d$) decreases from 4.85 to 3.83 eV when U is increased from 0 to 6 eV. We also note that for $U=6$ eV the unoccupied part of the f band has merged with the conduction band. The PDOS's in Figs. 2 and 3 indicate that there is a small admixture of Ce f states with the O $2p$ states at the top of the valence band as well as a small admixture of O $2p$ states with the occupied Ce f states (hybrydization). This phenomenon also exists for CeO_2 and has been reported to be a consequence of the nonorthogonality of the O $2p$ orbitals and Ce $4f$ states.[5] A way to lift this problem by using Wannier-type functions has been suggested in Ref. 5. Unfortunately, the practical applicability of this particular implementation[5] is not yet clear. Some improvements have been made to the approach in response to the criticism in Ref. 14. The authors of Ref. 14 pointed out the absence of the nonlinear core correction to the exchange-correlation energy in Ref. 5, which could result in erroneous overestimation of the exchange splitting. Taking such a correction into account has resulted in a better description of the ground state electronic structure of cerium oxide.[15] However, the disagreement with experimental thermodynamic data was sustained. In particular, the calculated reduction energy of CeO_2 is still strongly overestimated compared to experiment.[10] One should notice that the additional contribution compensating for the well-known failure of the density functional theory to correctly describe the O_2 binding energy (by 1.6–2.4 eV per oxygen molecule; see the discussion in Sec. III C) has been shown to worsen the agreement with experiment in Ref. 5, but was not applied in Ref. 10. On the other hand we note that the use of Wannier-type functions has only a minor effect on the total DOS. The GGA results (not shown) closely follow the LDA results in Figs. 2 and 3; however, for a fixed U the occupied f states of Ce_2O_3 are closer to the O $2p$ valence band edge. Moreover, the gap between the O $2p$ valence band edge and the conduction band is slightly higher in the GGA (4.01 eV for $U=5$ eV).

B. Structural properties of CeO_2 and Ce_2O_3

The lattice parameter increases linearly with U for CeO_2 (Fig. 4) and the reason for this behavior is a slight hybrydization of Ce $4f$ and O $2p$ orbitals. If the Ce $4f$ orbitals were completely unoccupied one would expect a to be independent of U. The increase of a as a function of U is almost the same for the LDA and the GGA. The experimental value[30] of 5.41 Å is obtained for $U \approx 6.6$ eV with the LDA, while the GGA always overestimates a by at least 0.05 Å. By construction the LDA generally underestimates the lattice parameter and the GGA often gives a slight overestimate.

In Figs. 5 and 6 we plot the equilibrium lattice parameters of Ce_2O_3, a and c/a, as functions of U. For $U \geqslant 1$ eV the results refer to the AFM ordering of the magnetic moments, and for $U=0$ eV to the FM ordering, i.e., to the corresponding lowest-energy solutions. Between $U=0$ and 2, especially close to $U=0$ eV, the curvature of a is more significant than that for $U>2$ eV. The decrease in curvature corresponds to

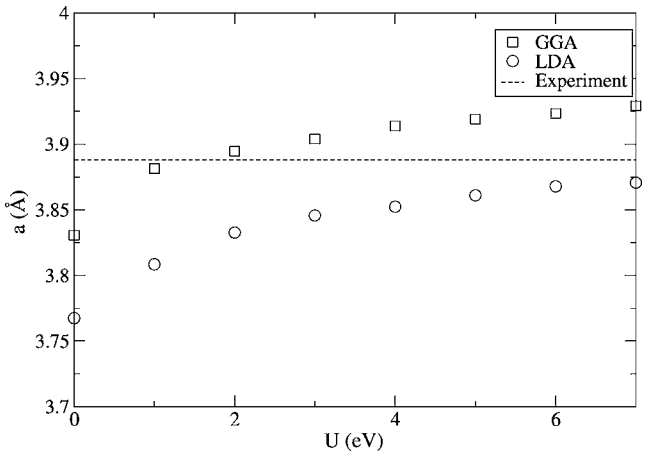

FIG. 5. The lattice parameter (a) of Ce_2O_3 as function of U. The horizontal line indicates the experimental value (Ref. 30).

the separation of the occupied f band from the unoccupied part, i.e., the transition from a metallic to an insulating solution that we discussed in Sec. III A. The c/a ratio shows similar U-dependent features as a. Below $U=2$ eV, c/a has an apparent curvature, but for $U>2$ eV c/a assumes a more or less constant value. Indeed, we do expect the localized or insulating solution to have a higher volume. The experimental values[30] are $a=3.888$ Å and $c/a=1.55$, which compare reasonably to both our LDA and GGA values above the metallic-insulating transition. As expected the GGA slightly overestimates the equilibrium cell volume and the LDA underestimates it.

Table I contains the bulk modulus B of CeO_2 and Ce_2O_3. Compared to experiments B of CeO_2 seems to be better described in the LDA than in the GGA. Unfortunately, there are no experimental data for Ce_2O_3.

C. Thermodynamic properties of CeO_2 and Ce_2O_3

Reduction of CeO_2 occurs via the reaction

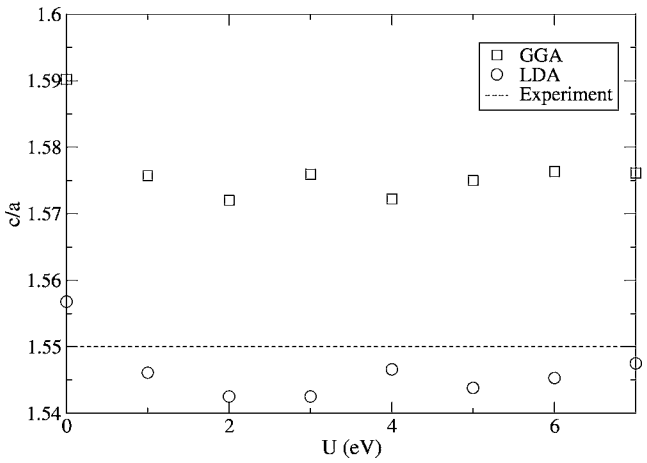

FIG. 6. The c/a ratio of Ce_2O_3 as function of U. The horizontal line indicates the experimental value (Ref. 30).

TABLE I. The bulk modulus B of CeO_2 and Ce_2O_3 for two different values of U. The values are in GPa.

	LDA		GGA		Expt.
	U (eV)				
	0	6	0	6	
CeO_2	205	214	175	186	236[a], 204[b]
Ce_2O_3	138	130	125	113	

[a]Reference 33.
[b]Reference 34.

$$CeO_2 \Leftrightarrow CeO_{2-x} + \frac{x}{2}O_2. \quad (2)$$

Eventually, reduction leads to formation of stoichiometric Ce_2O_3 and, thus, complete reduction corresponds to

$$2CeO_2 \Leftrightarrow Ce_2O_3 + \frac{1}{2}O_2. \quad (3)$$

The experimental reaction energy[31] of (3), $\Delta E_{Ce_2O_3}$, is 3.75 eV/Ce_2O_3 (estimated from thermodynamic data at $T=298$ K). Above the metallic-insulating transition, our calculated value of $\Delta E_{Ce_2O_3}$ (Fig. 7) decreases linearly for increasing values of U. The reason for this behavior is that a high U favors localization and thus facilitates the transition. Density functional theory is known to overestimate the binding energy of O_2 and this should result in an underestimation of $\Delta E_{Ce_2O_3}$ via the E_{O_2} term.[6] Consequently we cannot expect a perfect agreement with experiments for $\Delta E_{Ce_2O_3}$. However, as pointed out in Ref. 6 this error is independent of any conditions in the ceria material itself, i.e., it enters only through the E_{O_2} term. In the LDA the O_2 binding energy is overestimated by 1.2 eV/0.5 O_2 and in the GGA the corresponding number is 0.8 eV/0.5 O_2. The GGA always predicts a lower value of $\Delta E_{Ce_2O_3}$ than the LDA. From Fig. 7 we conclude that the experimental value of $\Delta E_{Ce_2O_3}$ corresponds

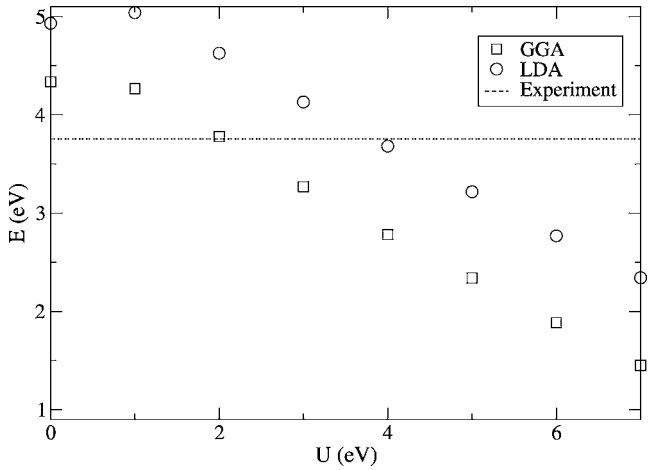

FIG. 7. The reaction energy of $2CeO_2 \Leftrightarrow Ce_2O_3 + (1/2)O_2$ as a function of U. The horizontal line indicates the experimental value (Ref. 31).

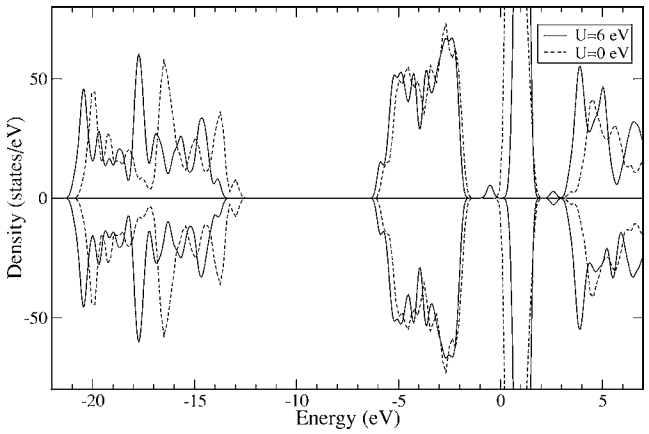

FIG. 8. The DOS of CeO_{2-x} obtained in the LDA for $U=0$ and 6 eV using Gaussian smearing (see Sec. II). The upper and lower panels show the spin-up and spin-down channels, respectively. The highest occupied state is at 0 eV. The small peak just below the Fermi level represents the localized f states. This peak is present only for $U=6$ eV.

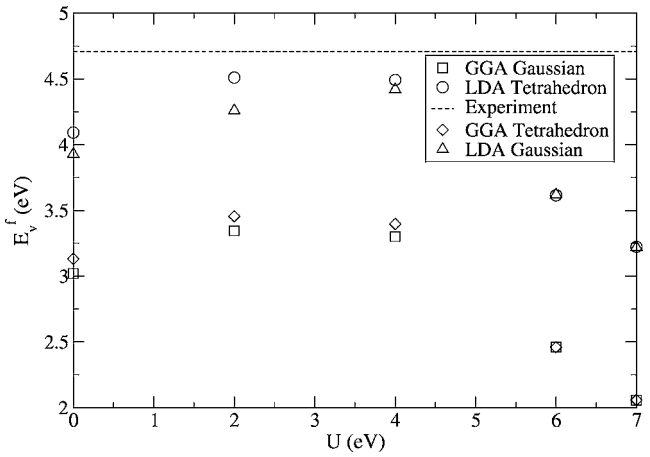

FIG. 9. The calculated vacancy formation energy (E_v^f) for different values of the Hubbard U. Two different methods for Brillouin-zone integration, labeled Gaussian and Tetrahedron, were used (see text). The experimental value is 4.72 eV (Ref. 32).

to $U\approx 2$ and ≈ 4 eV for the GGA and the LDA, respectively. However, in view of the uncertainties involved in the calculated value of E_{O_2} we conclude that U should be given larger values than $U\approx 2$ and ≈ 4 eV. In particular, we consider $\Delta E_{Ce_2O_3}$ obtained for $U\approx 6$ eV (LDA) and $U\approx 5$ eV (GGA), which are the U values suggested from a lattice parameter and an electronic structure point of view, as perfectly acceptable.

D. Partially reduced ceria CeO_{2-x}

We studied partially reduced ceria CeO_{2-x} by forming an oxygen vacancy in a $2\times 2\times 2$ supercell, which corresponds to $x=\frac{1}{32}$. According to the picture presented by Skorodumova *et al.*[3] two electrons localize on two nearest-neighbor Ce atoms, thus transforming into Ce^{3+}, when an oxygen vacancy forms. Starting from the DOS of CeO_2 in Fig. 1, upon reduction, we expect the occupied f states to appear as a peak in the band gap. If the localized f electrons are assumed to be ferromagnetically aligned the supercell should obtain a total magnetic moment of $\approx 2\mu_B$. The antiferromagnetic and ferromagnetic solutions are almost degenerate ($\Delta E<1$ meV) and in this work we assumed FM ordering.

Figure 8 shows the DOS of CeO_{2-x} for $U=0$ and 6 eV obtained with Gaussian smearing of 0.20 eV, used to improve visibility of the DOS structure. Clearly, localization of two f electrons, i.e., formation of two Ce^{3+} ions, occurs for $U=6$ eV but not for $U=0$ eV. By performing calculations for intermediate U values ($U=2$, 3, 4, and 5 eV) we conclude that a completely localized solution is obtained for $U=6$ or larger (LDA). For $U=6$ eV the distance between the O $2p$ valence band edge and the occupied f states is 1.4 eV, which was derived from calculations using the tetrahedron method for the Brillouin-zone integration. This value compares well with the experimental value of 1.2–1.5 eV.[27–29] By studying the PDOS we conclude that the two localized electrons occupy f orbitals on two Ce atoms that are nearest neighbors to the oxygen vacancy. A similar picture arises from the GGA, though the localized solution appears above $U=5$ eV instead of $U=6$ eV as for the LDA. Since CeO_{2-x} should be insulating with the occupied f states in the band gap, we argue that U must be chosen to satisfy this criterion, which implies $U\geqslant 6$ eV (LDA) or $U\geqslant 5$ eV (GGA). In fact the actual transition occurs between $U=5$ and 6 eV for the LDA; however, for the GGA the transition point is very close to $U=5$ eV.

From reaction (2) the vacancy formation energy is defined as

$$E_v^f = \frac{E_{CeO_{2-x}}}{x} + \frac{1}{2}E_{O_2} - \frac{E_{CeO_2}}{x}. \tag{4}$$

We have compiled the present results for E_v^f in Fig. 9. If Gaussian smearing with a smearing parameter of 0.20 eV is used to calculate E_v^f one finds excellent agreement with the tetrahedron method, which is supposedly more accurate, for the U values that yield localized f electrons. However for solutions that are not localized there are small errors. For $U=0$ eV, calculations using Gaussian smearing underestimate E_v^f by 0.16 eV (LDA) and 0.29 eV (GGA), respectively. For each U the E_v^f values were calculated for the equilibrium volume of CeO_2 corresponding to that particular U value. The experimental value is 4.72 eV,[32] though values between 4.65 and 5.00 eV have been reported for bulk reduction.[32] In correspondence with $\Delta E_{Ce_2O_3}$ [reaction (3)], the GGA underestimates E_v^f while the LDA provides a better estimate. The best agreement with the experimental value of E_v^f is obtained for $U=4$ eV in the LDA; however, in this case the solution is not localized. For $U=6$ eV we obtain a localized solution. In this case E_v^f deviates by ≈ 1 eV from the experimental value, which is expected from the uncertainties in the calculated value of E_{O_2} discussed above. Also, we note that the optimal U value for cerium oxides is close to the value for pure metallic Ce ($U=6.1$ eV and $J=0.7$ eV in the LDA).[35]

IV. CONCLUSIONS

We have studied how structural, thermodynamic, and electronic properties of CeO_2, Ce_2O_3, and CeO_{2-x} are described within the LDA+U formalism. Both the local density approximation and the generalized gradient approximation were applied and the $U-J$ parameter, labeled as U throughout this paper, was varied between 0 and 7 eV. From the study of the electronic structure we conclude that experimental data, i.e., band gaps and the position of the occupied f band with respect to the valence band edge, can be reasonably described with $U \approx 6$ eV in the LDA. The corresponding value in the GGA should be somewhat smaller, $U \approx 5$ eV, which agrees with previous theoretical studies.[6,10] In order to obtain the correct insulating ground state of CeO_{2-x} U must satisfy $U \geqslant 6$ eV (LDA) or $U \geqslant 5$ eV (GGA). This choice is further supported by the results for the structural parameters and reduction thermodynamics. In general the LDA seems to perform slightly better than the GGA. Reduction energies and vacancy formation energies deviate somewhat from experiments, but considering the known uncertainties this is definitely acceptable.

ACKNOWLEDGMENTS

We would like to thank VR and SSF for financial support. One of the authors (D.A.A.) gratefully acknowledges support from the Swedish Foundation for Strategic Research through the Center for Computational Thermodynamics (CCT) and the MATOP program. Additionally, we thank the Swedish National Infrastructure for Computing (SNIC) for computing resources. A. Lichtenstein is acknowledged for providing valuable discussion on the manuscript.

[1] H. Inaba and H. Tagawa, Solid State Ionics **83**, 1 (1996).
[2] A. Trovarelli, *Catalysis by Ceria and Related Materials* (Imperial College Press, London, 2002).
[3] N. V. Skorodumova, S. I. Simak, B. I. Lundqvist, I. A. Abrikosov, and B. Johansson, Phys. Rev. Lett. **89**, 166601 (2002).
[4] N. V. Skorodumova, R. Ahuja, S. I. Simak, I. A. Abrikosov, B. Johansson, and B. I. Lundqvist, Phys. Rev. B **64**, 115108 (2002).
[5] S. Fabris, S. de Gironcoli, S. Baroni, G. Vicario, and G. Balducci, Phys. Rev. B **71**, 041102(R) (2005).
[6] M. Nolan, S. C. Parker, and G. W. Watson, Surf. Sci. **595**, 223 (2005).
[7] M. Nolan, S. Grigoleit, D. C. Sayle, S. C. Parker, and G. W. Watson, Surf. Sci. **576**, 217 (2005).
[8] Y. Jiang, J. B. Adams, M. Schilfgaarde, R. Sharma, and P. A. Crozier Appl. Phys. Lett. **87**, 141917 (2005).
[9] Y. Jiang, J. B. Adams, and M. Schilfgaarde, J. Chem. Phys. **123**, 064701 (2005).
[10] S. Fabris, G. Vicario, G. Balducci, S. Gironcoli, and S. Baroni, J. Phys. Chem. B **109**, 22860 (2005).
[11] V. I. Anisimov, J. Zaanen, and O. K. Andersen, Phys. Rev. B **44**, 943 (1991).
[12] V. I. Anisimov, I. V. Solovyev, M. A. Korotin, M. T. Czyzyk, and G. A. Sawatzky, Phys. Rev. B **48**, 16929 (1993).
[13] S. L. Dudarev, G. A. Botton, S. Y. Savrasov, C. J. Humphreys, and A. P. Sutton, Phys. Rev. B **57**, 1505 (1998).
[14] G. Kresse, P. Blaha, J. L. F. Da Silva, and M. V. Ganduglia-Pirovano, Phys. Rev. B **72**, 237101 (2005).
[15] S. Fabris, S. de Gironcoli, S. Baroni, G. Vicario, and G. Balducci, Phys. Rev. B **72**, 237102 (2005).
[16] M. Cococcioni and S. de Gironcoli, Phys. Rev. B **71**, 035105 (2005).
[17] I. V. Solovyev and P. H. Dederichs, Phys. Rev. B **49**, 6736 (1994).
[18] G. Kresse and J. Hafner, Phys. Rev. B **48**, 13115 (1993).
[19] G. Kresse and J. Furthmüller, Comput. Mater. Sci. **6**, 15 (1996).
[20] G. Kresse and J. Furthmüller, Phys. Rev. B **54**, 11169 (1996).
[21] G. Kresse and D. Joubert, Phys. Rev. B **59**, 1758 (1999).
[22] P. E. Blöchl, Phys. Rev. B **50**, 17953 (1994).
[23] J. P. Perdew, J. A. Chevary, S. H. Vosko, K. A. Jackson, M. R. Pederson, D. J. Singh, and C. Fiolhais, Phys. Rev. B **46**, 6671 (1992).
[24] H. J. Monkhorst and J. D. Pack, Phys. Rev. B **13**, 5188 (1976).
[25] P. E. Blöchl, O. Jepsen, and O. K. Andersen, Phys. Rev. B **49**, 16223 (1994).
[26] E. Wuilloud, B. Delley, W.-D. Schneider, and Y. Baer, Phys. Rev. Lett. **53**, 202 (1984).
[27] D. R. Mullins, P. V. Radulovic, and S. H. Overbury, Surf. Sci. **429**, 186 (1999).
[28] A. Pfau and K. D. Schierbaum, Surf. Sci. **321**, 71 (1994).
[29] M. A. Henderson, C. L. Perkins, M. H. Engelhard, S. Thevuthasan, and C. H. F. Peden, Surf. Sci. **526**, 1 (2003).
[30] L. Eyring, in *Handbook on the Physics and Chemistry of Rare Earths*, edited by K. A. Gschneider and L. Eyring (North-Holland, Amsterdam, 1979), Vol. 3, Chap. 27.
[31] I. Barin, O. Knacke, and O. Kubaschewski, *Thermochemical Properties of Inorganic Substances* (Springer-Verlag, Dusseldorf, 1973), Supplement.
[32] M. A. Panhans and R. N. Blumwnthal, Solid State Ionics **60**, 279 (1993).
[33] L. Gerward and J. S. Olsen, Powder Diffr. **8**, 127 (1993).
[34] A. Nakajima, A. Yoshihara, and M. Ishigame, Phys. Rev. B **50**, 13297 (1994).
[35] A. B. Shick, W. E. Picket, and A. I. Liechtenstein, J. Electron Spectrosc. Relat. Phenom. **114**, 753 (2001).